

# ILDR1 promotes influenza A virus replication through binding to PLSCR1

Yueyue Liu<sup>1</sup>, Shuqian Lin<sup>2</sup>, Yunhui Xie<sup>2</sup>, Lu Zhao<sup>2</sup>, Haibo Du<sup>1</sup>, Shifa Yang<sup>2</sup>, Bin Yin<sup>2</sup>, Guiming Li<sup>2</sup>, Zengcheng Zhao<sup>2</sup>, Zhongli Huang<sup>2</sup>, Zhigang Xu<sup>1</sup>, and Jiaqiang Wu<sup>1</sup>

<sup>1</sup>Shandong University School of Life Science

<sup>2</sup>Shandong Academy of Agricultural Sciences

April 16, 2024

## Abstract

As a natural antiviral regulator, phospholipid scramblase 1 (PLSCR1) has been shown to inhibit influenza virus replication in infected cells through interacting with NP of influenza A virus (IAV). But its antiviral function as well as the underlying regulatory mechanism has not been examined *in vivo*. In the present work, we show that PLSCR1 expression is decreased in H1N1 SIV-infected mice, and *Plscr1*<sup>-/-</sup> mice are more susceptible to H1N1 SIV infection. By performing yeast two-hybrid screening, we identified immunoglobulin-like domain-containing receptor 1 (ILDR1) as a novel PLSCR1-binding partner. ILDR1 is highly expressed in the lungs, and its expression level is increased after virus infection. Interestingly, ILDR1 could not directly interact with virus NP protein, but could combine with PLSCR1 competitively. Our data indicates that there is a previously unidentified PLSCR1-ILDR1-NP regulatory pathway playing a vital role in limiting IAV infection, which provides novel insights into IAV-host interactions.

## Introduction

Influenza A virus (IAVs), which contains eight negative single-strand RNA segments, could facilitate new virus through gene reassortment or mutation, such as the 2009 pandemic H1N1 in human that caused serious deaths and economic losses (Vincent A, 2014). Between 2011 and 2018, a predominant emergent EA reassortant genotype 4 (G4) virus in pigs had pdm/09 and TR-derived internal genes and showed increasing human infectivity (Sun, 2020). The virial RNA (vRNA) is bound to RNA-dependent RNA polymerase complex (RdRp) and encapsidated by the nucleoprotein (NP), forming the so-called viral ribonucleoprotein (vRNP) complex (Lamb, 1983). The vRNP is the key to IAV life cycle and important for viral pathogenicity and host range determinants (Davis, 2017). NP is essential for the translocation of vRNP into the nucleus of host cells and could be used as a target to block the replication of influenza virus specifically (Ozawa, 2007; Cros, 2005). A series of host proteins have been reported to regulate nuclear entry through interacting with NP, such as  $\alpha$ -actinin-4 (Sharma, 2014), CRM1 (Pickens, 2018), UAP56 (Chiba, 2018), Hsp40 (Batra, 2016) and MOV10 (Zhang, 2016), hence played important roles in promoting or inhibiting virus replication. So, identification of new NP-binding host proteins will help to provide new targets for prevention and/or control of influenza viruses.

Phospholipid scramblase 1 (PLSCR1) was first identified as a calcium-binding type II membrane protein that could be induced by (Li, 2016). It is involved in multiple biological processes, such as gene transcription regulation, cell proliferation, differentiation and apoptosis (Gui, 2020; Huang, 2020; Li, 2006; Stray, 2005). Recently, the antiviral activity of PLSCR1 received extensive attentions. PLSCR1 inhibits HBV infection and replication through mediating ubiquitin-dependent degradation of HBx protein (Yuan, 2015), and mediates resistance of HCV infection through interfering with the viral entry into host cells (Gong, 2011). PLSCR1



pfu H1N1 SIV to infect C57BL/6J mice intranasally and examined PLSCR1 levels at different time points post infection. The results show that PLSCR1 expression is markedly decreased when examined at 1 day post infection (dpi) (Figure 1D). PLSCR1 expression continues to decrease to less than 5% at 5 dpi, then gradually returns to the normal level by 14 dpi (Figure 1D and 1E). This dynamic change of PLSCR1 expression suggests that PLSCR1 might play an essential role in SIV infection *in vivo*. **Figure 1. PLSCR1 Expression after H1N1 SIV Infection.** (A) The similarity of PLSCR1 between different species. (B) The identity percentage of nucleoprotein of influenza virus between the isolated strain from the diseased pigs and human. (C) Western blots showed that PLSCR1 expression in various tissues of C57BL/6 mice on day 42. (D) PLSCR1 and ILDR1 protein levels in lung are modulated after swine influenza A virus (SIV) infection. The lungs were dissected from C57BL/6J mice that were either mock- or SIV-infected at multiple days p.i. as indicated. (E and F) The area of the PLSCR1 and ILDR1 peak, in relation to the standard curve, was determined using ImageJ software. Bars represent mean  $\pm$  s.d. \* $P < 0.05$  \*\* $P < 0.01$ ; \*\*\* $P < 0.001$ .

### H1N1 SIV replication is increased in *Plscr1* knockout mice

In order to investigate the functions of PLSCR1 during Influenza A virus infection *in vivo*, we developed *Plscr1* knockout mice using CRISPR/Cas9 genome editing technique. The mouse *Plscr1* gene contains eight exons encoding 378 amino acids, and two sgRNAs were designed to target exon 4 (Figure 2A). DNA sequencing revealed that a deletion of 122 bp was introduced into exon 4 in *Plscr1* knockout mice, which causes a premature translational stop and gives rise to a potentially truncated protein of 43 amino acids (Figure 2B). RT-PCR, western blot, and immunohistochemistry results confirm that PLSCR1 expression is indeed disrupted in the homogenous knockout mice (Figures 2C-2E). Interbreeding of *Plscr1*<sup>+/-</sup> mice gave rise to offspring in the expected Mendelian ratio (23.8% wild-type, 47.6% *Plscr1*<sup>+/-</sup>, and 28.6% *Plscr1*<sup>-/-</sup>; n=42) with normal viability, suggesting that PLSCR1 is dispensable for general development in mice.

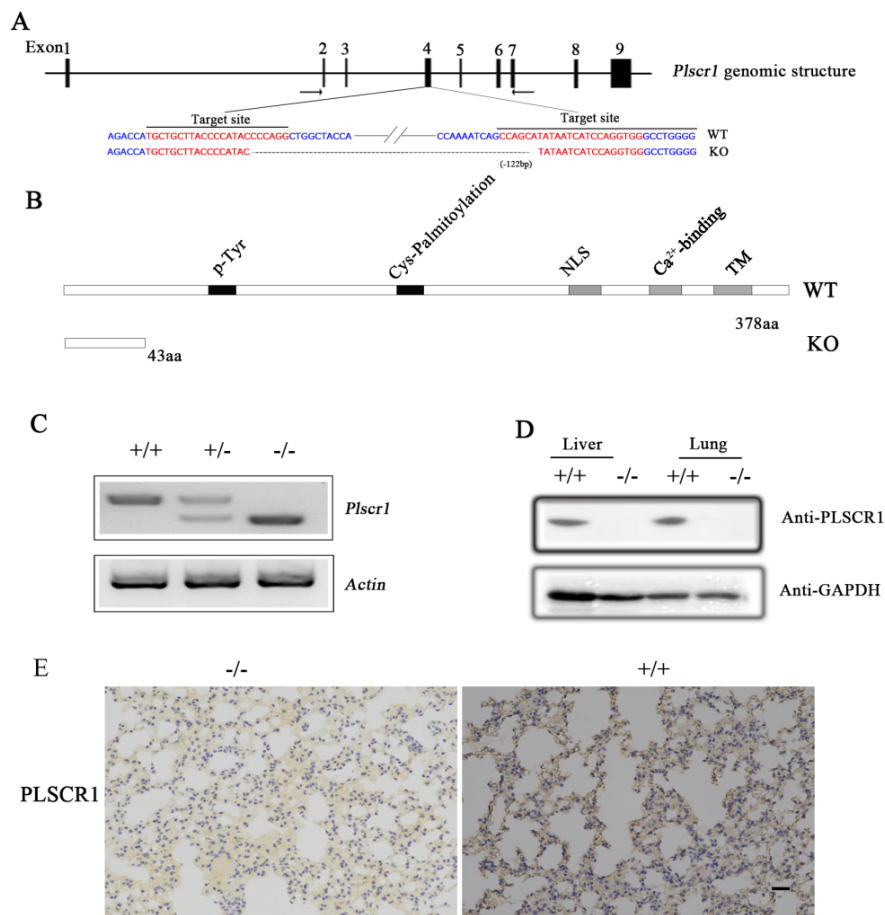


**Figure 2. Construction of *Plscr1* knockout mice.** (A) The schematic drawing of the strategy for *Plscr1* gene disruption. The target sites of clustered regularly interspaced short palindromic repeat (CRISPR)-Cas9 small guide RNAs (sgRNAs) in the *Plscr1* gene are indicated in red, and the deleted region in the *Plscr1* gene of knockout mice is indicated by dashes. The positions of RT-PCR primers are indicated by arrows. (B) The schematic drawing of the domain structure of PLSCR1 in wildtype and knockout mice. (C) The expression of *Plscr1* mRNA in the tail of P42 mice was determined by RT-PCR.  $\beta$ -actin was included as the internal control. (D) Western blot showed the expression in the liver and lung of P42 mice. (E) PLSCR1 was detected by immunohistology using rabbit anti-mPLSCR1, visualized with 3,3'-diaminobenzidine, and counterstained with hematoxylin. Scale bar: 20  $\mu$ m. +/+ : wild type mice; +/- : heterozygous mice; -/- : *Plscr1* knockout mice.

We then examined whether *Plscr1* knockout affects H1N1 SIV infection. Control and *Plscr1*<sup>-/-</sup> mice were infected intranasally with 10<sup>3</sup> pfu H1N1 SIV, and the survival rate, body weight and lung virus load were determined over a 28-day period. The results show that the survival rate of *Plscr1*<sup>-/-</sup> mice is much lower than that of control mice after SIV infection (Figure 3A). *Plscr1*<sup>-/-</sup> mice start to die at 3 dpi, and the survival rate drops to 50% at 28 dpi. Meanwhile, similar body weight was observed between survived *Plscr1*<sup>-/-</sup> mice and control mice (Figure 3B). Consistent with the decreased survival rate, higher lung viral load was observed in *Plscr1*<sup>-/-</sup> mice (Figure 3C). Titers of SIV increase in the lungs of both genotypes and peak at 5 dpi, then start to decrease and not detectable at 14 and 28 dpi. Virus titers are significantly higher in *Plscr1*<sup>-/-</sup> mice at all time points examined (Figure 3C). Consistently, western blotting shows that the level of NP in *Plscr1*<sup>-/-</sup> mice was significantly higher than that in wild mice at 3 dpi (Figure 3D and 3E). Taken together, our present data suggest that H1N1 SIV replication is increased in *Plscr1* knockout mice that leads to lower

survival rate.

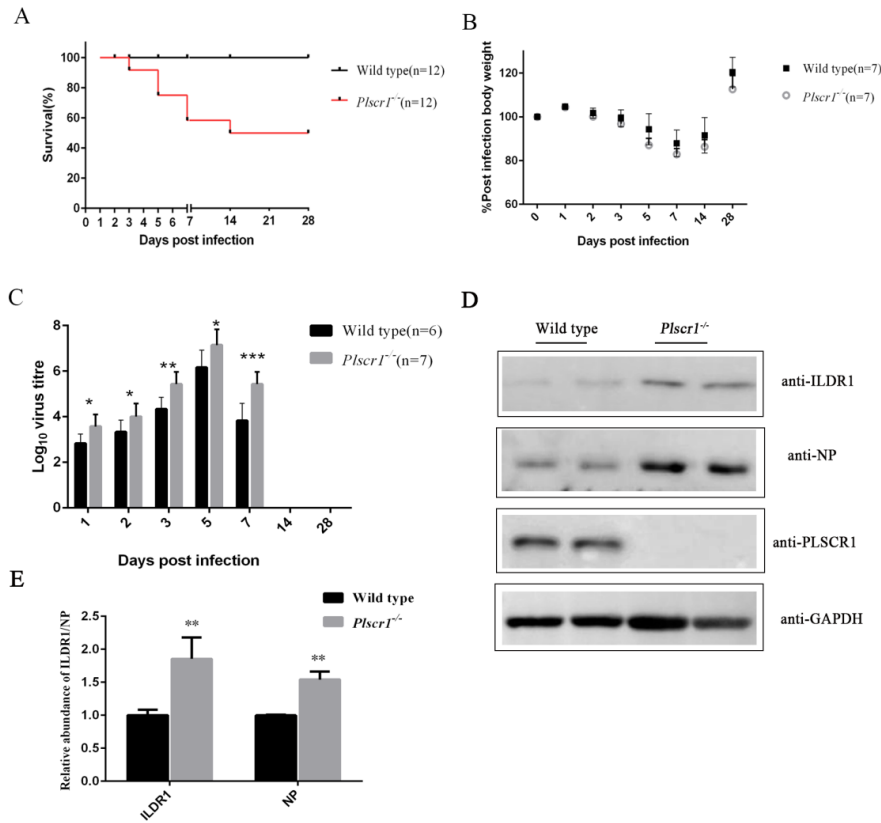


Figure 3. PLSCR1 influences the infection of mice by Swine influenza virus (SIV). (A) C57BL/6J and *Plscr1*<sup>-/-</sup> mice were infected intranasally with 10<sup>3</sup> pfu. SIV. Suviral was determined daily and calculated as a percentage of the initial total numbers. (B) Mice were weighed daily and the weights represented as a percentage of the starting weight (n=7 per group). (C) Lung tissues were taken at multiple days p.i. as indicated and virus titer determined by plaque assay (n>6 per group). Data represent the mean value±SD. Asterisks indicate statistical difference (Unpaired t test, \*P<0.05, \*\*P<0.01, \*\*\*P<0.001). (D) Western blots showed that ILDR1 and NP protein expression in lung of C57BL/6 and *Plscr1*<sup>-/-</sup> mice on day 42 after infected with 10<sup>3</sup> p.f.u. SIV for 3 days. (E) Statistical analysis of ILDR1 and NP levels in *Plscr1*<sup>-/-</sup> mice. The value for ILDR1 and NP were standardized to the GAPDH level and normalized to the level of ILDR1 and NP in lung of wild type mice. Data are shown

as the means SD from three independent experiments (Unpaired t test, \*P<0.05, \*\*P<0.01, \*\*\*P<0.001).

### ILDR1 is a novel PLSCR1-binding protein

In our previous study, we performed yeast two-hybrid screening of a chicken cDNA library using the C-terminal intracellular domain of ILDR1 (228–553 aa) as bait (Liu et al., 2017). Among the positive clones identified, five clones encode PLSCR1. We then performed co-immunoprecipitation (co-IP) experiments to confirm the interaction between ILDR1 and PLSCR1. The results show that EGFP-tagged mouse ILDR1 cytoplasmic domain could be co-immunoprecipitated together with Myc-tagged PLSCR1 (Fig. 4A). Likewise, EGFP-tagged PLSCR1 could be co-immunoprecipitated together with Myc-tagged ILDR1 cytoplasmic domain (Fig. 4B). ILDR1-EGFP mainly localizes in the cytoplasm in COS-7 cells as reported previously (Fig. 4C) (Hauge et al., 2004). In contrast, PLSCR1-mCherry localizes in both cytoplasm and nucleus (Fig. 4D). When cotransfected, ILDR1-EGFP translocates from cytoplasm to nuclei with PLSCR1-Mcherry (Fig.

4E). Our co-IP and co-localization results suggest that ILDR1 is a novel PLSCR1-binding partner.

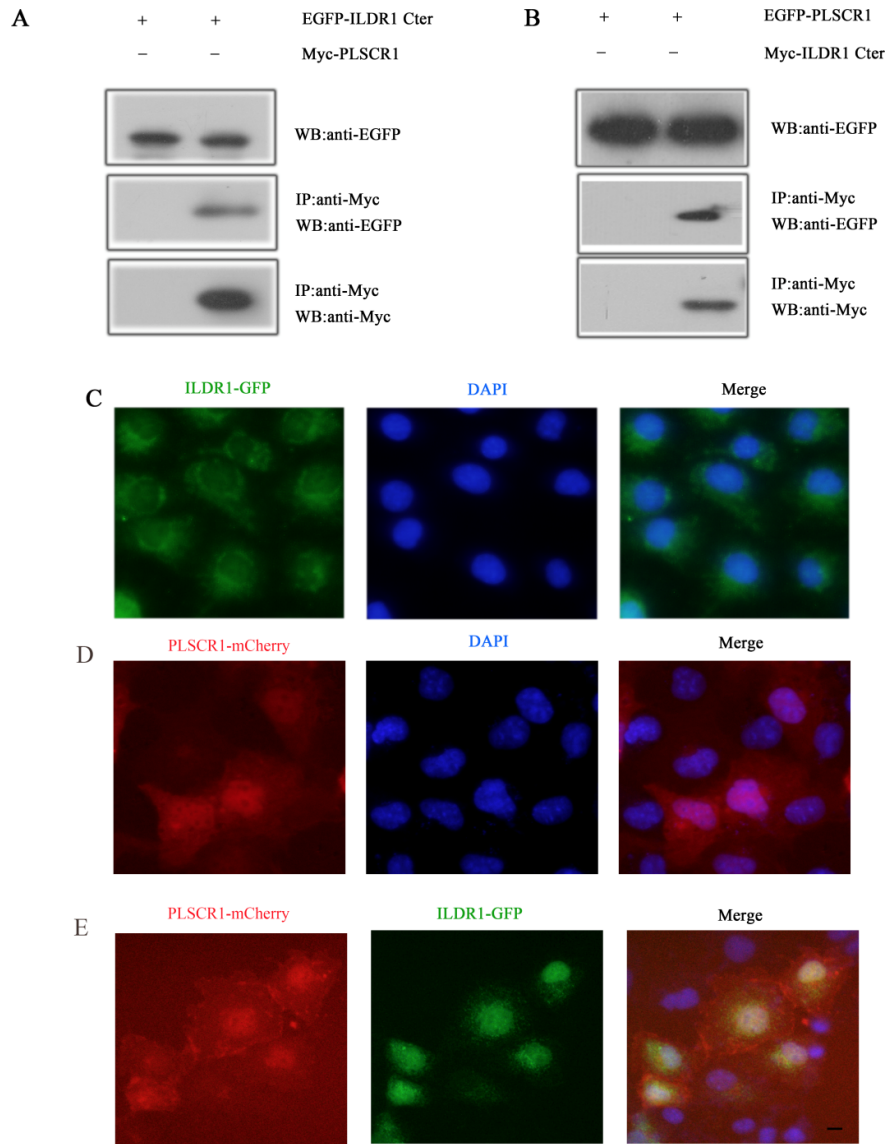


**Figure 4. PLSCR1 binds ILDR1.** (A) Western blots showing that EGFP-tagged cytoplasmic fragment of ILDR1 was co-immunoprecipitated with Myc-tagged PLSCR1. (B) Western blots showing that EGFP-tagged PLSCR1 was co-immunoprecipitated with Myc-tagged cytoplasmic fragment of ILDR1. Expression vectors were transfected into HEK293T cells to express epitope-tagged proteins, and cell lysis were subject to immunoprecipitation. 5% of total protein was loaded as input. IP indicates antibody used for immunoprecipitation and WB indicates antibody used for detection. (C) ILDR1-EGFP localize in the cytoplasm of COS7. (D) PLSCR1-mCherry localize in the cytoplasm of COS7. (E) However, when PLSCR1-mCherry is present, ILDR1-GFP translocates into the nuclei. Expression vectors were transfected into COS-7 cells to express epitope-tagged proteins. Nuclei were stained with DAPI. Scale bar: 10  $\mu$ m.

#### ILDR1 promotes H1N1 SIV infection in cultured cells

In order to explore the role of ILDR1 in influenza virus infection, we first determined the level of ILDR1

in C57BL/6J mice after H1N1 SIV infection. Western blot results show that ILDR1 level is significantly increased by more than 15-fold on the first day after infection and then decreases as the viral load decreases (Figures 1D and 1F). ILDR1 expression was also examined by performing immunohistology. ILDR1 is weakly expressed in the lungs of mice before infection, while a substantial increase of ILDR1-positive cells was observed at 3 dpi (Figure 5A and 5B). The quantitative analysis shows a 3–6-fold ( $P < 0.05$ ) increase in the percentage area stained in the lungs at 3 dpi. ILDR1 levels was restored to a normal level on 14 dpi (Figure 5A and 5B). In addition, ILDR1 levels in *Plscr1*<sup>-/-</sup> mice were examined after SIV infection at 3 dpi. The results show that ILDR1 expression is up-regulated after viral infection in *Plscr1*<sup>-/-</sup> mice, suggesting that ILDR1 might play a role in Influenza virus infection (Figure 3D).

We next analyzed the effect of ILDR1 on SIV infection in HEK 293T cells. qRT-PCR results reveal that the expression of *ILDR1* mRNA is significantly increased after SIV infection in a dosage- and time-dependent way (Figures 5B and 5C). To examine the effect of ILDR1 overexpression, HEK293T cells were transfected with ILDR1-expressing vector or empty vector, followed by infection with SIV at an MOI of 0.1. The results show that SIV TCID<sub>50</sub> and viral RNA are significantly increased in ILDR1-overexpressing cells (Figures 5D and 5F). Meanwhile, the viability of virus-infected cells is significantly decreased in ILDR1-overexpressing cells (Figure 5E). Taken together, our present data suggest that ILDR1 promotes H1N1 SIV infection.

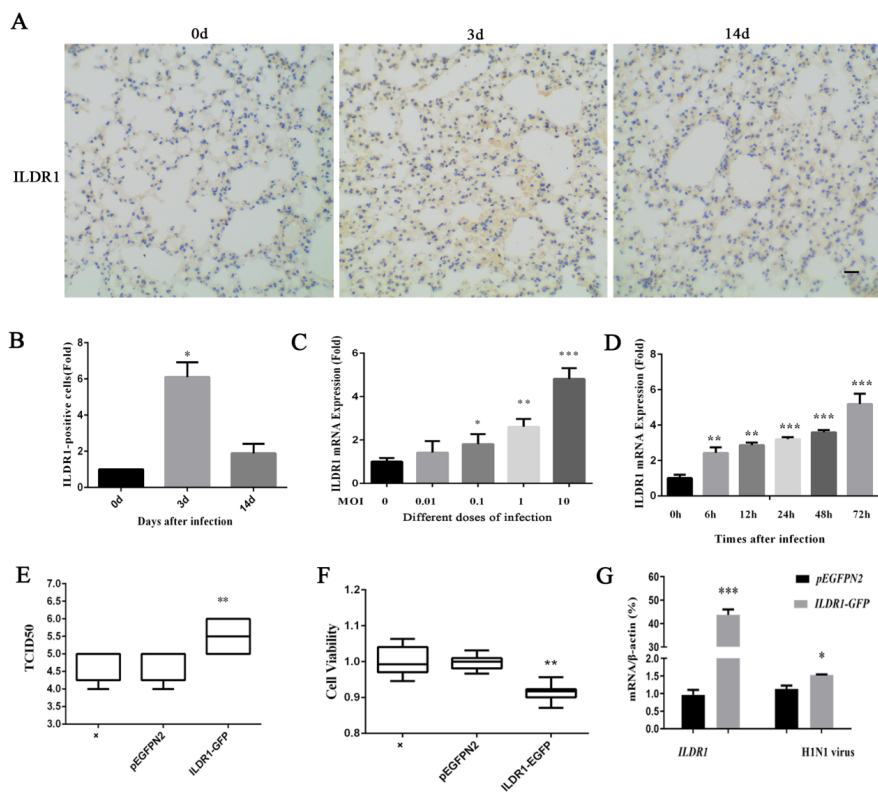


**Figure 5. ILDR1 Expression after swine influenza virus infection.** (A) The lungs of mice were taken after infection 0, 3 and 14 days for immunohistochemical detection. ILDR1 was detected by immunohistology using rabbit anti-ILDR1, visualized with 3,3'-diaminobenzidine and counterstained with hematoxylin. Scale bar: 20  $\mu$ m. The expression levels of the ILDR1 after infection relative to that of normal expression were analyzed by areal density (B). (C) HEK 293T cells were infected with different doses (MOI=0, 0.01, 0.1, 1, 10) for 48h, and supernatants were collected, then the expression of *ILDR1* was confirmed by quantitative reverse-transcription PCR. Data represent the mean value  $\pm$  SD. Asterisks indicate statistical difference (Unpaired t test; \* $P < 0.05$ , \*\* $P < 0.01$ , \*\*\* $P < 0.001$ ). (D) Expression of *ILDR1* in virus-infected cells at an MOI of 0.1. The

supernatants were collected at different time points (0h, 6h, 12h, 24h, 48h) and subjected to RT-qPCR. Data represent the mean value $\pm$ SD. Asterisks indicate statistical difference (Unpaired t test; \*P<0.05, \*\*P<0.01, \*\*\*P<0.001). (E) Virus replication in ILDR1-overexpressing HEK293T cells. Cells were transduced with ILDR1-GFP or pEGFPN2 for 24h, and then infected with SIV at an MOI of 0.1. Supernatants were collected at the indicated timepoints, and virus titers or NP expression were determined by TCID50, CCK-8 (F) and RT-qPCR (G).

### **ILDR1 competes with NP in binding PLSCR1**

We transfected either ILDR1-Cter or PLSCR1 together with NP protein in HEK 293T cells and examined their potential interaction by performing co-IP experiments. The results show that Myc-tagged PLSCR1 but not ILDR1-Cter is co-immunoprecipitated with EGFP-tagged NP protein (Figure 6A). Likewise, EGFP-tagged PLSCR1 but not ILDR1-Cter is co-immunoprecipitated with Myc-tagged NP (Figure 6B). We then moved on to examine whether ILDR1 and NP could interact with PLSCR1 simultaneously or compete with each other. We examined the interaction between NP and PLSCR1 in the presence of ILDR1 of increasing amounts. The results show that when the amount of ILDR1 is increased, the level of NP bound to PLSCR1 is decreased (Figures 6C and 6D). Similar results were obtained when increasing amounts of NP was used (Figures 6E and 6F).

In order to further verify that ILDR1 and PLSCR1 will affect the nuclear importation of NP, a cell fractionation experiment was conducted. Cells were transduced with ILDR1-GFP, PLSCR1-Myc or empty retrovirus-transduced control for 24h, and then infected with SIV at an MOI of 0.1. At 6 h p.i., the cells were separated into nuclear (N) and cytoplasmic fractions (C), then subjected to western blotting. The results show that, GAPDH and LaminB1 were only detected in the cytoplasm and nucleus, respectively. Also we found that NP was primarily detected in the cytoplasm and was only weakly detected in the nucleus while PLSCR1 was overexpressed as reported previously[21]. In contrast, when we overexpressed ILDR1, it will promote the expression of NP protein into the nucleus. When ILDR1 and PLSCR1 were co-transfected, a considerable amount of NP was detected in both the nucleus and the cytoplasm (Figures 6G). Taken together, our present data suggest that ILDR1 and NP compete with each other in binding PLSCR1.

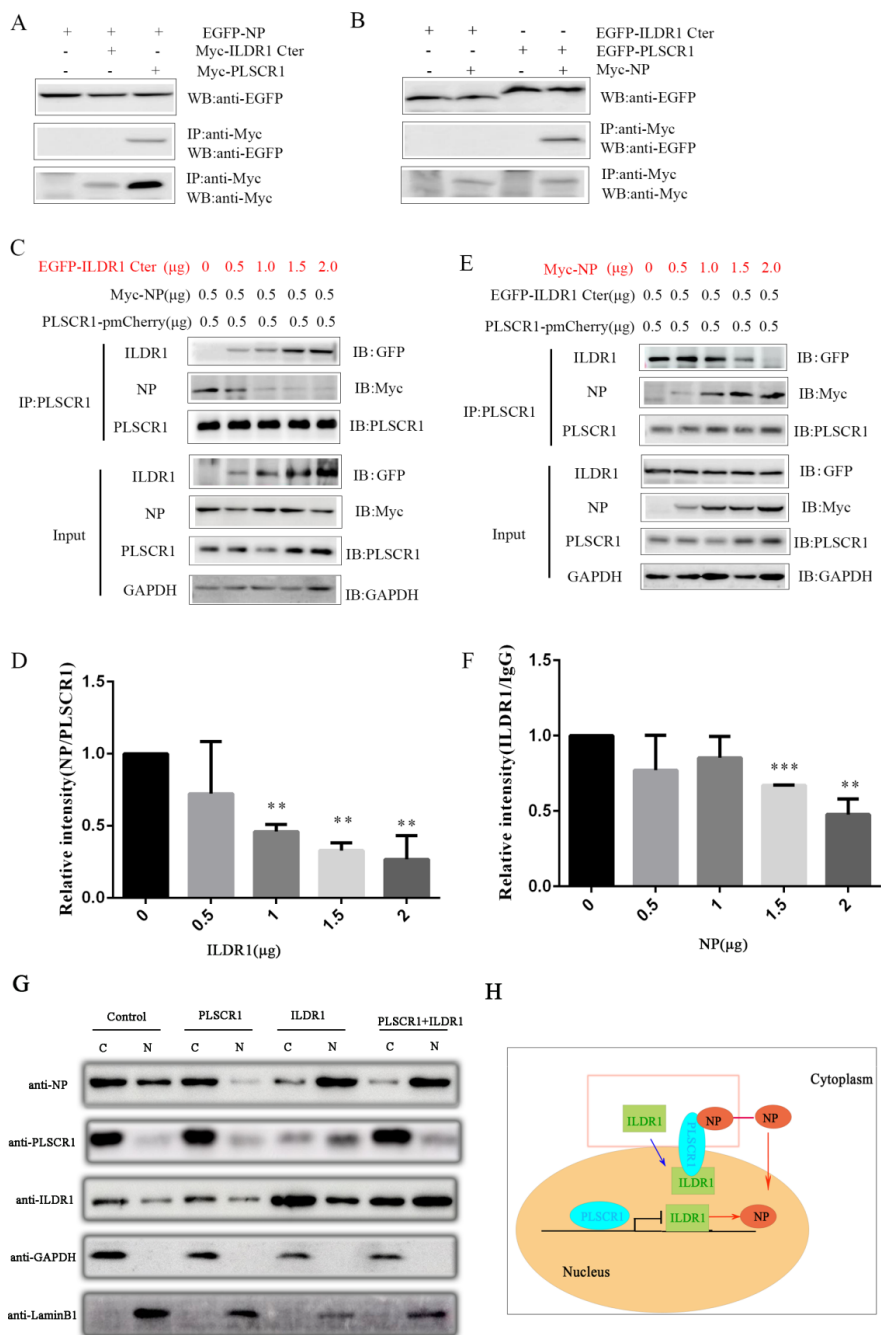


**Fig 6. The viral PLSCR1-NP interaction is competitively by ILDR1.** (A,B) No interaction of ILDR1 with viral NP as determined by the co-IP assays. The interaction between the ILDR1 Cter domain and the NP of SIV was validated using the co-IP assays. HEK293T cells were transfected with ILDR1 and NP protein. The Myc-tagged PLSCR1 plasmids were used as positive controls. All cell lysates were prepared at 24 h post transfection and proteins were immunoprecipitated using an anti-Myc mouse MAb, or anti-EGFP rabbit MAb. The immunoprecipitated proteins were analyzed by Western blotting. (C) HEK293T cells were transfected with Myc-NP (0.5 μg), PLSCR1-pmCherry (0.5 μg) and different concentrations of EGFP-ILDR1 cytoplasmic fragment (0 μg, 0.5 μg, 1 μg, 1.5 μg, 2 μg). The cell lysates were prepared, and proteins were

immunoprecipitated using an anti-PLSCR1 rabbit PAb. The expression levels of the ILDR1 and NP protein after immunoprecipitation relative to that of GAPDH were analyzed by densitometry(D). (E) HEK293T cells were transfected with EGFP-ILDR1 cytoplasmic fragment (0.5 $\mu$ g) , PLSCR1-pmCherry (0.5 $\mu$ g) and different concentrations of Myc-NP (0 $\mu$ g,0.5 $\mu$ g,1 $\mu$ g,1.5 $\mu$ g,2 $\mu$ g) .The cell lysates were prepared, and proteins were immunoprecipitated using an anti-PLSCR1 rabbit PAb. The expression levels of the ILDR1 and NP protein after immunoprecipitation relative to that of GAPDH were analyzed by densitometry(F).(G) Cells were transduced with ILDR1-GFP ,PLSCR1-Myc or empty retrovirus-transduced control for 24h, and then infected with SIV at an MOI of 0.1. At 6 h p.i., the cells were separated into nuclear (N) and cytoplasmic fractions (C). Each fraction was subjected to western blotting with corresponding antibody for protein detection.(H) Model of PLSCR1-NP interaction is competitively by ILDR1.ILDR1 located in the cytoplasm, when in the presence of PLSCR1, ILDR1 and PLSCR1 co-translocates into the nuclei . PLSCR1 could prevent the nuclear import of NP protein and ILDR1 could bind to PLSCR1competitively with NP. So in the nuclei ,PLSCR1 inhibit the expression of ILDR1 to reduce NP protein synthesis to inhibit virus replication .

## Discussion

Influenza A virus has caused several outbreaks of influenza in human history, including the 2009 H1N1 Influenza pandemics. As a single-strand negative-strand, segmented RNA virus, its high mutation rate and gene rearrangement properties can continuously produce new virus subtypes, imposing a long-term threat to human and animal health. Swine have receptors for both human influenza (SA $\alpha$ -2,6-Gal) and avian influenza (SA $\alpha$ -2,3-Gal), hence are referred to as "mixers" of influenza viruses (Castrucci, 1993). They play an important role in the recombination of influenza viruses. In 2009, the H1N1pdm09 IV pandemic broke out in the world, and researchers found that many of its gene fragments are derived from SIV(Vincent ,2014). In addition, the H1N1 subtype SIV has always maintained a high prevalence rate in the pig herd (Sadler, 2011), and has been involved in the recombination of a variety of new viruses during its evolution (Zimmermann, 2011). The experimental strain used in the present work was collected from a sick pig farm, and shows homology of more than 90% with the 2009 human epidemic strains. Therefore, our work is of great significance for exploring the pathogenic mechanism of H1N1.

Influenza A virus ribonucleoprotein (vRNP) complex is the structural basis of viral RNA transcription and replication, and plays an important role in the process of virus infection (Chutiwitoonchai , 2016). During the early stage of viral infection, the vRNP complex is released into the cytoplasm of the host cell via endocytosis and demembrane, and then enters the nucleus with the help of nuclear localization signals and transport proteins (Wang, 1997). To date, several host proteins have been reported to be potential binding partners of the vRNP complex, and regulate viral infection through various mechanisms (Davis ,2017). For example, PLSCR1 negatively regulates virus replication by interacting with NP in the cytoplasm and preventing its nuclear import *in vitro* (Luo, 2018). In our present work, we established *Plscr1* knockout mice and found that it is indeed more susceptible to SIV. By examining the survival rate, body weight and lung virus load of the mice, we presented *in vivo* evidence for the first time that PLSCR1 is important for inhibiting influenza virus replication.

Moreover, we identified ILDR1 as a novel PLSCR1-binding partner. ILDR1 has been shown to mediate fat-stimulated cholecystokinin (CCK) secretion (Chandra ,2013) and play an important role in regulating the integration of tTJs(Higashi ,2015). *Ildr1* knockout mice show profound hearing loss accompanied with tTJs destruction in the inner ear (Mehrjoo ,2015; Morozko ,2015) and polyuria due to renal concentrating defects in kidneys (Hempstock ,2020). ILDR1 is a putative type I transmembrane protein containing an immunoglobulin (Ig)-like domain (Hauge ,2004). ILDR1 belongs to angulin protein family, which also includes immunoglobulin-like domain-containing receptor 2 (ILDR2) and lipolysis-stimulated lipoprotein receptor (LSR). The immunomodulatory effect of its homologous protein ILDR2 has been extensively studied in recent years. It has been confirmed that ILDR2 is a new B7 family protein, expressed in immune cells and inflammatory tissues, and has the activity of suppressing T cells (Hecht ,2018). ILDR2-Fc regulates the function of immunity in the treatment of autoimmune diseases by regulating the stability of the immune

internal environment and rebuilding the balance of immune tolerance (Podojil ,2018).In our previous study, we detected high expression of ILDR1 in lungs of mice (Liu, 2017). However, its function in the lungs and whether it participates in disease infection has not been reported so far. Therefore, we observed the role of ILDR1 in influenza virus infection. We first determined the level of ILDR1 after H1N1 SIV infection by western blot and immunohistochemistry. The results showed that ILDR1 levels significantly increased by more than 15-fold on the first day after infection and it decreased as the viral load decreased. The same results were obtained using *Plscr1* knockout mice. Moreover, we examined the effect of ILDR1 overexpression on virus infection, and confirmed that virus replication was significantly promoted and the viability of virus-infected cells is decreased, suggesting that ILDR1 might play a role in Influenza virus replication.

ILDR1 could interact with PLSCR1, which has been reported to impair nuclear import of influenza A virus NP. To explore whether ILDR1 affects virus infection through regulating NP importation, we first detected the interaction between ILDR1 and NP using co-IP. The results show that PLSCR1 could interact with NP protein as previously reported, but ILDR1 could not directly interact with NP. Then, the effect of ILDR1 and NP on PLSCR1 was determined, and we found that they could bind NP protein competitively. At present it remains unclear why ILDR1 affects the replication of influenza virus, and what role does it play in other virus? Further investigation is needed to clarify the mechanism by which ILDR1 regulates viral replication.

## Materials and Methods

**Animals.** Generation of *Plscr1* Knockout mice were generated using the clustered regularly interspaced short palindromic repeat (CRISPR)-associated Cas9 nuclease (CRISPR/Cas9) genome editing technique as previously described(Yang , 2013). Briefly, C57BL/6 female mice (7–8 weeks old) were superovulated by intraperitoneally injecting pregnant mare serum gonadotropin (PMSG) and human chorionic gonadotrophin (hCG) and then mated to C57BL/6 male mice. The fertilized embryos (zygotes) were collected from the oviducts, and mixed Cas9 mRNA (50 ng/μl) and small guide RNA (sgRNA; 25 ng/μl) were injected into the cytoplasm of zygotes with visible pronuclei in Chatot-Ziomek-Bavister (CZB) medium. The injected zygotes were then cultured in Quinn’s Advantage cleavage medium (in vitro Fertilization, Inc.) for 24 h, at which time 18–20 2-cell-stage embryos were transferred into the oviduct of a pseudopregnant ICR female mouse at 0.5 day post coitus (dpc). The accession numbers of the *Plscr1* cDNAs used to design sgRNA is NM\_011636.2. To determine the nucleotide sequence of mutated alleles, genomic DNA of F0 mice was amplified using the following primers: forward, 5′ -GGTGATCTCGATT CAGGGGT-3′ , reverse, 5′ -GGGGTTACTCGACCCTAAAA -3′. DNA sequencing was then performed after TA cloning into plasmid pMD19T. In order to obtain F1 knockout mice, F0 mice were crossed with C57BL/6 mice and newborns were examined by Sanger sequencing .All animal experiments were approved by the Shandong Academy of Agricultural Science and conducted accordingly. All methods were performed in accordance with the relevant guidelines and regulations.

**Virus.** SIV(QD-2018 strain) was a H1N1 strain that isolated and obtained from the diseased pigs in Shandong province of China, which can be used as one of representative strains for the analysis of variant strains. The virus was continuously passaged on MDCK cells and virus titer was as high as  $10^{4.5}$  TCID<sub>50</sub>/mL.

**Cell culture, transfection.** HEK 293T ,COS7 and A549 cells were maintained with 10% FBS DMEM medium at 37°C under 5% CO<sub>2</sub>, and transfected with expression vectors or siRNAs using Lipofectamine 2000 Transfection Reagent (thermofisher) according to the manufacturer’s instructions.

**Plasmid construction.** The cDNAs encoding the mouse *Ildr1* and *Plscr1* were cloned into pmCherry-N1, pEGFP-C2, and pMyc-C2 (modified pEGFP-C2 with EGFP-coding sequence replaced by Myc-coding sequence) as we have reported. All the constructs were verified by Sanger sequencing.

**Western blot.** Cultured cells were transfected with expression vectors as described above or siRNAs synthesized by the Sigma-Aldrich company, then protein was resuspended with RIPA cell lysis containing 1 mM PMSF (Beyotime; Shanghai, China). After centrifuging at 4 for 20 min, the supernatant was analyzed by western blot. Protein samples were resolved by 10% SDS-PAGE, then transferred to a PVDF membrane. Af-

ter blocking with 5% BSA buffer for 1 h, the membrane was incubated with Rabbit Polyclonal-PLSCR1 Polyclonal Antibody (Proteintech, Cat#11582-1-AP,1:1000 diluted), Rabbit Polyclonal-Anti-ILDR1 antibody (Abcam, Cat#ab89847,1:1000 diluted), Rabbit Polyclonal-Anti-H1N1 Influenza A virus Nucleocapsid protein antibody(Abcam,Cat#ab104870,1:1500 diluted), rabbit anti-GAPDH antibody(Abcam,Cat.#ab181602, 1:5000 diluted), rabbit anti-LaminB1 antibody(Abways,Cat.#AB0054, 1:3000 diluted) at 4 over night, followed by incubation with goat anti-mouse secondary antibody or goat anti-rabbit secondary (Cell Signaling Technology, Danvers, MA) at room temperature for two hours. The signals were detected with the ECL system (Cell Signaling Technology, Danvers, MA).

**RNA extraction, RT-PCR and Quantitative real-time PCR.** Total RNA was isolated from virus-infected cells or mouse tissues and cDNA was carried out by reverse transcription (RT) following the kit instructions (TaKaRa Bio Inc., Dalian, China). The expression of gene or virus was analyzed by quantitative real-time PCR (SYBR(r) Premix Ex Taq™ system, Takara). The primers used were as follows: *Ildr1* forward primer, CCGGCGGCTGATGAAGAAAGACTC, reverse primer, AGGGCAGCAACAGCGGGTAGGA;*Plscr1* forward primer, GTGGGGCGTC TAGACCTTTC, reverse primer, CCAGGCATCACAGGTGAGTT; H1N1 forward primer, ACAGAAGTTATAAGAATGA, reverse primer, TGTCTCCGAAGAAAT AAGA; $\beta$ -actin forward primer, ACGGCCAGGTCATCACTATTG, reverse primer, AGGGGCCGACTCATCGTA. PCR reaction system and procedures were referred to Premix Taq kit instructions (Takara). PCR reaction sets were adjusted between 24 and 36 cycles, and annealing temperatures were adjusted between 55 and 60 °C. The PCR products were separated by electrophoresis on agarose gel.

Quantitative real-time PCR was carried out using SYBR® Premix Ex Taq™ system (Perfect Real Time, Takara). The primers and template were the same as that used in RT-PCR. Amplification and detection were run in a Roche 480 Sequence Detection System with an initial cycle of 95 °C for 10 s followed by 40 cycles of 95 °C for 5 s, 62 °C for 10 s and 72 °C for 5 s. All PCR reactions were performed in triplicate. Fold change in gene expression level was calculated using the  $2^{-\Delta\Delta C_t}$  method and all PCR reactions were performed in triplicate.

**Immunofluorescence assay.** Infected cells or transfected cells with GFP- or mCherry-tagged proteins growing on Gelatin-coated glass cover slips were fixed with 4% paraformaldehyde (PFA) in PBS for 15 min and blocked with PBT1 buffer (0.1% Triton X-100, 1% BSA, 5% heat-inactivated goat serum in PBS, pH 7.3) for 30 min. Cells were incubated overnight at 4°C with corresponding diluted in PBT1 then washed twice with PBS for 10 min. And cells were incubated with FITC-conjugated secondary antibody diluted in PBT2 (0.1% Triton X-100, 0.1% BSA in PBS) for 1 h, followed by washing with PBS three times for 10 min. For nuclei staining, cells were incubated with DAPI (Solarbio Life Sciences) for 15 min, followed by three 10 min PBS washes, then mounted in 50% glycerol/PBS. The cells were imaged with an inverted fluorescence microscope(TE200, Nikon).

**Immunohistochemistry.** The tissues were fixed in 10% formalin solution, embedded in paraffin, sectioned to 4  $\mu$ m thicknesses and dewaxed the paraffin sections to water. Then the sections were placed in a retrieval box filled with EDTA antigen retrieval buffer (PH8.0) in a microwave oven for antigen retrieval. After that, the sections were blocked with 5% BSA for 30 min at room temperature. The section were incubated with anti-PLSCR1 antibody (1:50) overnight at 4°C. After a brief wash, the secondary antibody were used for detection at room temperature for 50 min and DAPI dye solution was added for 10 min in the dark. The images were taken using a light microscopy (Nikon Eclipse C1). For the controls, no antibody was added to the samples.

**Cell fractionation.** The PLSCR1-overexpressing or empty retrovirus-transduced control A549 cells grown in 6-well plates were infected with WSN virus at an MOI of 5. At 6 h p.i., the cells were separated into nuclear and cytoplasmic fractions by using Minute Nuclear and Cytoplasmic Extraction Reagents (SC-003, Invent) according to the manufacturer's procedure. The amount of NP, ILDR1 and PLSCR1 in each fraction were determined by western blotting with a rabbit anti-NP pAb, a rabbit anti-ILDR1 pAb and a rabbit anti-PLSCR1 pAb, respectively. LaminB1 and GAPDH, nuclear and cytoplasmic fraction markers,

respectively, were detected by western blotting with a rabbit anti-GAPDH pAb and a rabbit anti-LaminB1 pAb, respectively.

**Co-immunoprecipitation (co-IP).** HEK293T cells were transfected with expression vectors as described above, then washed twice with PBS 24 h after transfection and resuspended in ice-cold lysis buffer containing 150 mM NaCl, 50 mM Tris at pH 7.5, 0.1% Triton X-100, and 1×cocktail (Roche, Basel, Switzerland). After centrifuging at 4°C for 20 min, the supernatant was collected and incubated with immobilized anti-Myc or anti-EGFP antibody at 4°C overnight. Immunoprecipitated proteins were washed three times with 300 mM lysis buffer and then analyzed by western blot.

**Statistical analyses.** All data were expressed as means ± standard deviation (SD), and an independent-sample *t*-test was used to evaluate data using Graph Prism software. \**p*<0.05, \*\**p*<0.01, \*\*\**p*<0.001.

### Conflict of Interest Statement

The authors declare that the research was conducted in the absence of any commercial or financial relationships that could be construed as a potential conflict of interest.

### Acknowledgments

This study was funded by National Natural Science Funds(32070178),Shandong Provincial Modern Agricultural Industry and Technology System (SDAIT-08-06), Shandong Province Agriculture Major Application Technology Innovation Project(SD2019XM007),Talent Engineering Projects (ts201511069; W03020496), Agricultural Science and Technology Innovation Project of Shandong Academy of Agricultural Sciences(CXGC2021A12 and CXGC2021A15) ,Independent training innovation team of Jinan (2019GX-RC025) and National Key Research and Development Program of China (2017YFC1702700).

### REFERENCES

1. Vincent A, Awada L, Brown I, Chen H, Claes F, Dauphin G, Donis R, Culhane M, Hamilton K, Lewis N, Mumford E, Nguyen T, Parchariyanon S, Pasick J, Pavade G, Pereda A, Peiris M, Saito T, Swenson S, Van Reeth K, Webby R, Wong F, Ciacci-Zanella J. (2014). *Review of influenza A virus in swine worldwide: a call for increased surveillance and research*. Zoonoses Public Health, 61(1):4-17. doi: 10.1111/zph.12049.
2. Sun H, Xiao Y, Liu J, Wang D, Li F, Wang C, Li C, Zhu J, Song J, Sun H, Jiang Z, Liu L, Zhang X, Wei K, Hou D, Pu J, Sun Y, Tong Q, Bi Y, Chang KC, Liu S, Gao GF, Liu J. (2020). *Prevalent Eurasian avian-like H1N1 swine influenza virus with 2009 pandemic viral genes facilitating human infection*. Proc Natl Acad Sci, 117(29):17204-17210. doi: 10.1073/pnas.1921186117.
3. Lamb RA, Choppin PW. (1983). *The gene structure and replication of influenza virus*. Annu Rev Biochem, 52:467-506. doi: 10.1146/annurev.bi.52.070183.002343.
4. Davis AM, Ramirez J, Newcomb LL. (2017). *Identification of influenza A nucleoprotein body domain residues essential for viral RNA expression expose antiviral target*. J Virol,14(1):22. doi: 10.1186/s12985-017-0694-8.
5. Ozawa M, Fujii K, Muramoto Y, Yamada S, Yamayoshi S, Takada A, Goto H, Horimoto T, Kawaoka Y. (2007). *Contributions of two nuclear localization signals of influenza A virus nucleoprotein to viral replication*. J Virol, 81(1):30-41. doi: 10.1128/JVI.01434-06.
6. Cros JF, García-Sastre A, Palese P. (2005). *An unconventional NLS is critical for the nuclear import of the influenza A virus nucleoprotein and ribonucleoprotein*. Traffic, 6(3):205-13. doi: 10.1111/j.1600-0854.2005.00263.x.
7. Sharma S, Mayank AK, Nailwal H, Tripathi S, Patel JR, Bowzard JB, Gaur P, Donis RO, Katz JM, Cox NJ, Lal RB, Farooqi H, Sambhara S, Lal SK. (2014). *Ινφλυενζα Α ιραλ νυςλεοπροτειν ιντερακτις ωπη ςψτοσκελετον ςαφφολδινγ προτειν α-αστινιν-4 φορ ιραλ ρεπλιςατιον*.FEBS J, 281(13):2899-914. doi: 10.1111/febs.12828.
8. Pickens JA, Tripp RA. (2018). *Verdinexor Targeting of CRM1 is a Promising Therapeutic Approach against RSV and Influenza Viruses*.Viruses, 10(1):48. doi: 10.3390/v10010048.

9. Chiba S, Hill-Batorski L, Neumann G, Kawaoka Y. (2018). *The Cellular DExD/H-Box RNA Helicase UAP56 Co-localizes With the Influenza A Virus NS1 Protein*. *Front Microbiol*, 9:2192. doi: 10.3389/fmicb.2018.02192.
10. Batra J, Tripathi S, Kumar A, Katz JM, Cox NJ, Lal RB, Sambhara S, Lal SK. (2016). *Human Heat shock protein 40 (Hsp40/DnaJB1) promotes influenza A virus replication by assisting nuclear import of viral ribonucleoproteins*. *Sci Rep*, 6:19063. doi: 10.1038/srep19063.
11. Zhang J, Huang F, Tan L, Bai C, Chen B, Liu J, Liang J, Liu C, Zhang S, Lu G, Chen Y, Zhang H. (2016). *Host Protein Moloney Leukemia Virus 10 (MOV10) Acts as a Restriction Factor of Influenza A Virus by Inhibiting the Nuclear Import of the Viral Nucleoprotein*. *J Virol*, 90(8):3966-3980. doi: 10.1128/JVI.03137-15.
12. Li Q, Zhang B, Zhang Q, Wang X, Huo Y, Yang J. (2016). *Effect of PLSCR1 on the Antiviral Activity of IFN against HBV in HepG2 Cells*. *Bing Du Xue Bao*, 32(6):747-51. Chinese. PMID: 30004207.
13. Stray SJ, Bourne CR, Punna S, Lewis WG, Finn MG, Zlotnick A. (2005). *A heteroaryldihydropyrimidine activates and can misdirect hepatitis B virus capsid assembly*. *Proc Natl Acad Sci*, 102(23):8138-43. doi: 10.1073/pnas.0409732102.
14. Li YF, Wang GF, He PL, Huang WG, Zhu FH, Gao HY, Tang W, Luo Y, Feng CL, Shi LP, Ren YD, Lu W, Zuo JP. (2006). *Synthesis and anti-hepatitis B virus activity of novel benzimidazole derivatives*. *J Med Chem*, 49(15):4790-4. doi: 10.1021/jm060330f.
15. Gui L, Zhu YW, Xu Q, Huang JJ, Hua P, Wu GJ, Lu J, Ni JB, Tang H, Zhang LL. (2020). *RNA interference-mediated downregulation of phospholipid scramblase 1 expression in primary liver cancer in vitro*. *Oncol Lett*, 20(6):361. doi: 10.3892/ol.2020.12225.
16. Huang P, Liao R, Chen X, Wu X, Li X, Wang Y, Cao Q, Dong C. (2020). *Nuclear translocation of PLSCR1 activates STAT1 signaling in basal-like breast cancer*. *Theranostics*, 10(10):4644-4658. doi: 10.7150/thno.43150.
17. Yuan Y, Tian C, Gong Q, Shang L, Zhang Y, Jin C, He F, Wang J. (2015). *Interactome map reveals phospholipid scramblase 1 as a novel regulator of hepatitis B virus x protein*. *J Proteome Res*, 14(1):154-63. doi: 10.1021/pr500943x.
18. Gong Q, Cheng M, Chen H, Liu X, Si Y, Yang Y, Yuan Y, Jin C, Yang W, He F, Wang J. (2011). *Phospholipid scramblase 1 mediates hepatitis C virus entry into host cells*. *FEBS Lett*, 585(17):2647-52. doi: 10.1016/j.febslet.2011.07.019.
19. Zhu J, Sheng J, Dong H, Kang L, Ang J, Xu Z. (2013). *Phospholipid scramblase 1 functionally interacts with angiogenin and regulates angiogenin-enhanced rRNA transcription*. *Cell Physiol Biochem*, 32(6):1695-706. doi: 10.1159/000356604.
20. Dong B, Zhou Q, Zhao J, Zhou A, Harty RN, Bose S, Banerjee A, Slee R, Guenther J, Williams BR, Wiedmer T, Sims PJ, Silverman RH. (2004). *Phospholipid scramblase 1 potentiates the antiviral activity of interferon*. *J Virol*, 78(17): 8983-93. doi: 10.1128/JVI.78.17.8983-8993.
21. Luo W, Zhang J, Liang L, Wang G, Li Q, Zhu P, Zhou Y, Li J, Zhao Y, Sun N, Huang S, Zhou C, Chang Y, Cui P, Chen P, Jiang Y, Deng G, Bu Z, Li C, Jiang L, Chen H. (2018). *Phospholipid scramblase 1 interacts with influenza A virus NP, impairing its nuclear import and thereby suppressing virus replication*. *PLoS Pathog*, 14(1):e1006851. doi: 10.1371/journal.ppat.1006851.
22. Higashi T, Katsuno T, Kitajiri S, Furuse M. (2015). *Deficiency of angulin-2/ILDR1, a tricellular tight junction-associated membrane protein, causes deafness with cochlear hair cell degeneration in mice*. *PLoS One*, 10(3):e0120674. doi: 10.1371/journal.pone.0120674.
23. Liu Y, Nie H, Liu C, Zhai X, Sang Q, Wang Y, Shi D, Wang L, Xu Z. (2017). *Angulin proteins ILDR1 and ILDR2 regulate alternative pre-mRNA splicing through binding to splicing factors TRA2A, TRA2B, or SRSF1*. *Sci Rep*, 7(1):7466. doi: 10.1038/s41598-017-07530-z.
24. Yu Z, Cheng K, He H, Wu J. (2020). *A novel reassortant influenza A (H1N1) virus infection in swine in Shandong Province, eastern China*. *Transbound Emerg Dis*, 67(1):450-454. doi: 10.1111/tbed.13360.
25. Hauge H, Patzke S, Delabie J, Aasheim HC. (2004). *Characterization of a novel immunoglobulin-like domain containing receptor*. *Biochem Biophys Res Commun*, 323(3):970-8. doi: 10.1016/j.bbrc.2004.08.188.

26. Castrucci MR, Donatelli I, Sidoli L, Barigazzi G, Kawaoka Y, Webster RG. (1993). *Genetic reassortment between avian and human influenza A viruses in Italian pigs*. *Virology*, 193(1):503-6. doi: 10.1006/viro.1993.1155.
27. Sadler AJ, Williams BR. (2011). *Dynamiting viruses with MxA*. *Immunity*, 35 (4):491-3. doi: 10.1016/j.immuni.2011.10.005.
28. Zimmermann P, Mänz B, Haller O, Schwemmler M, Kochs G. (2011). *The viral nucleoprotein determines Mx sensitivity of influenza A viruses*. *J Virol*, 85(16):8133-40. doi: 10.1128/JVI.00712-11.
29. Chutiwitoonchai N, Aida Y. (2016). *NXT1, a Novel Influenza A NP Binding Protein, Promotes the Nuclear Export of NP via a CRM1-Dependent Pathway*. *Viruses*, 8(8):209. doi: 10.3390/v8080209.
30. Wang P, Palese P, O'Neill RE. (1997). *The NPI-1/NPI-3 (karyopherin alpha) binding site on the influenza A virus nucleoprotein NP is a nonconventional nuclear localization signal*. *J Virol*, 71(3):1850-6. doi: 10.1128/JVI.71.3.1850-1856.
31. Chandra R, Wang Y, Shahid RA, Vigna SR, Freedman NJ, Liddle RA. (2013). *Immunoglobulin-like domain containing receptor 1 mediates fat-stimulated cholecystokinin secretion*. *J Clin Invest*, 123(8):3343-52. doi: 10.1172/JCI68587.
32. Morozko EL, Nishio A, Ingham NJ, Chandra R, Fitzgerald T, Martelletti E, Borck G, Wilson E, Rioridan GP, Wangemann P, Forge A, Steel KP, Liddle RA, Friedman TB, Belyantseva IA. (2015). *ILDR1 null mice, a model of human deafness DFNB42, show structural aberrations of tricellular tight junctions and degeneration of auditory hair cells*. *Hum Mol Genet*, 24(3):609-24. doi: 10.1093/hmg/ddu474.
33. Mehrjoo Z, Babanejad M, Kahrizi K, Najmabadi H. (2015). *Two novel mutations in ILDR1 gene cause autosomal recessive nonsyndromic hearing loss in consanguineous Iranian families*. *J Genet*, 94(3):483-7. doi: 10.1007/s12041-015-0537-6.
34. Hempstock W, Sugioka S, Ishizuka N, Sugawara T, Furuse M, Hayashi H. (2020). *Angulin-2/ILDR1, a tricellular tight junction protein, does not affect water transport in the mouse large intestine*. *Sci Rep*, 10(1):10374. doi: 10.1038/s41598-020-67319-5.
35. Hecht I, Toporik A, Podojil JR, Vaknin I, Cojocaru G, Oren A, Aizman E, Liang SC, Leung L, Dicken Y, Novik A, Marbach-Bar N, Elmesmari A, Tange C, Gilmour A, McIntyre D, Kurowska-Stolarska M, McNamee K, Leitner J, Greenwald S, Dassa L, Levine Z, Steinberger P, Williams RO, Miller SD, McInnes IB, Neria E, Rotman G. (2018). *ILDR2 Is a Novel B7-like Protein That Negatively Regulates T Cell Responses*. *J Immunol*, 200(6): 2025-2037. doi: 10.4049/jimmunol.1700325. Epub 2018 Feb 5. PMID: 29431694.
36. Podojil JR, Hecht I, Chiang MY, Vaknin I, Barbiro I, Novik A, Neria E, Rotman G, Miller SD. (2018). *ILDR2-Fc Is a Novel Regulator of Immune Homeostasis and Inducer of Antigen-Specific Immune Tolerance*. *J Immunol*, 200(6): 2013-2024. doi: 10.4049/jimmunol.1700326.
37. Yang H, Wang H, Shivalila CS, Cheng AW, Shi L, Jaenisch R. (2013). *One-step generation of mice carrying reporter and conditional alleles by CRISPR/Cas-mediated genome engineering*. *Cell*, 154(6):1370-9. doi: 10.1016/j.cell.2013.08.022.